

*N*²-Aroylanthranilamide Inhibitors of Human Factor Xa

Ying K. Yee,* Anne Louise Tebbe, Jared H. Linebarger, Douglas W. Beight, Trelia J. Craft, Donetta Gifford-Moore, Theodore Goodson, Jr., David K. Herron, Valentine J. Klimkowski, Jeffrey A. Kyle, J. Scott Sawyer, Gerald F. Smith, Jennifer M. Tinsley, Richard D. Towner, Leonard Weir, and Michael R. Wiley*

Lilly Research Laboratories, Eli Lilly & Company, Indianapolis, Indiana 46285

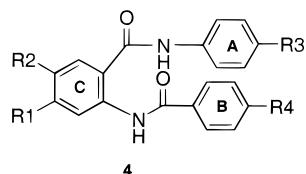
Received June 24, 1999

Reversal of the A-ring amide link in 1,2-dibenzamidobenzene **1** (fXa $K_{\text{ass}} = 0.81 \times 10^6$ L/mol) led to a series of human factor Xa (hfXa) inhibitors based on *N*²-aroylanthranilamide **4**. Expansion of the SAR around **4** showed that only small planar substituents could be accommodated in the A-ring for binding to the S1 site of hfXa. Bulky groups such as 4-isopropyl, 4-*tert*-butyl, and 4-dimethylamino were favored in the B-ring to interact with the S4 site of hfXa. The central (C) ring containing a 5-methanesulfonamido group yielded greater activity than carbamoyl groups. Combining the beneficial features from the B- and C-ring SAR, compound **55** represents the most potent hfXa inhibitor in the *N*²-aroylanthranilamide **4** series with hfXa $K_{\text{ass}} = 58 \times 10^6$ L/mol ($K_i = 11.5$ nM).

Introduction

Discovery of selective human factor Xa inhibitors (hfXa) is of great interest as a treatment for thromboembolic disorders.^{1–3} There are several potential advantages of a safe and orally effective hfXa inhibitor over the current treatments, as described in our previous paper.⁴ For example, coumadin has a narrow therapeutic index and its prophylactic treatment carries a bleeding liability. As a result, patients undergoing treatment with coumadin require regular monitoring. These deficiencies provided the impetus to search for safer and more effective anticoagulant agents.

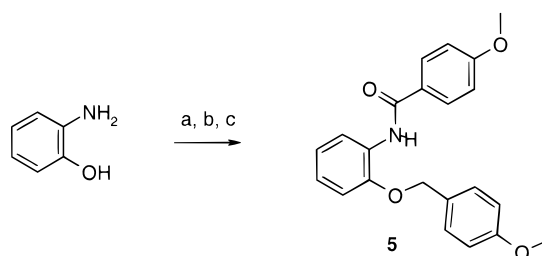
hfXa is upstream from thrombin in the amplification of the coagulation cascade. Inhibition of hfXa instead of thrombin could be more effective in attenuating the coagulation cascade. The previous paper in this series describes the discovery of 1,2-dibenzamidobenzenes such as **1–3** (Table 1), which are novel inhibitors of hfXa with neutral S1 and S4 binding elements.⁴ The current goal was to discover more structurally diverse leads which could serve as starting points for future modifications to improve oral absorption. In this account, we report our early efforts to develop inhibitors of hfXa related to **1** with alternative linkers connecting the central ring to the S1 and S4 binding elements. These studies led to the identification of a new series of anthranilamides (**4**) which retain high affinity for hfXa.



Chemistry

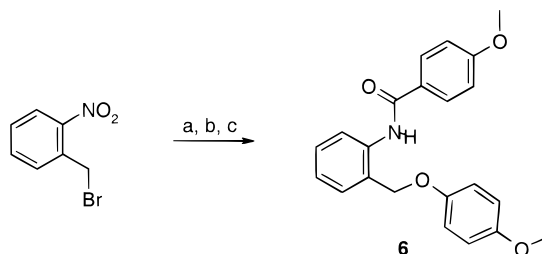
In our initial studies on alternative linkers for connecting the central ring to the S1 and S4 binding

Scheme 1^a



^a Reagents: (a) 2 equiv *p*-anisoyl chloride, TEA; (b) 5 N NaOH, MeOH; (c) *p*-MeOBnCl, DMF, K₂CO₃, acetone.

Scheme 2^a

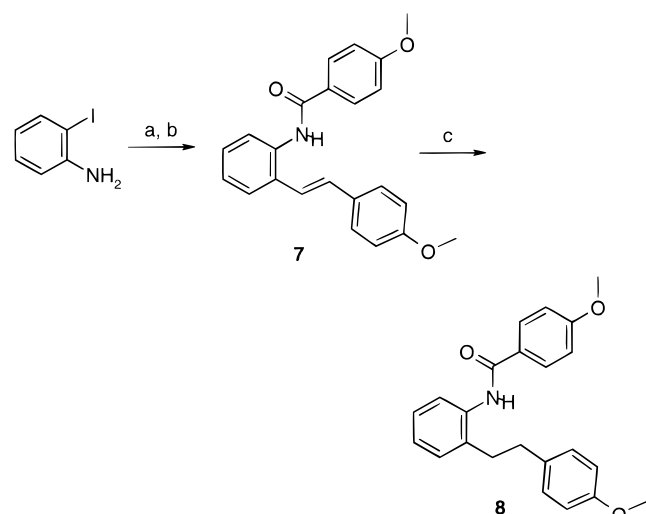


^a Reagents: (a) 2 equiv *p*-MeOPhOH, KOtBu; (b) H₂ 10% Pd/C, THF; (c) *p*-anisoyl chloride, pyridine.

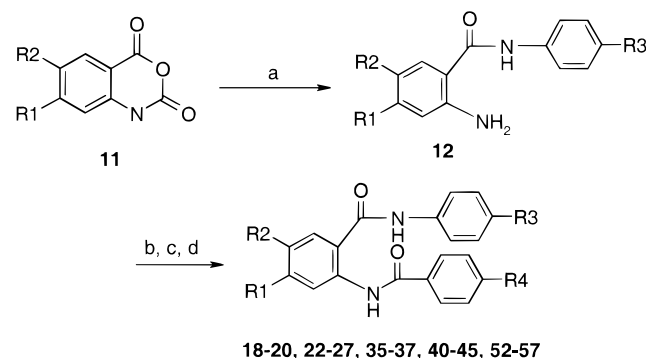
elements, *p*-anisole groups were used for both A- and B-rings. Preparation of compounds containing an ether linkage (**5** and **6**, Table 2) was achieved by a Williamson synthesis (Schemes 1 and 2). The unsaturated *trans*-vinylene linker **7** was constructed by a Heck coupling reaction (Scheme 3).⁵ Compound **7** was hydrogenated to provide the saturated ethylene-linked analogue **8**. The diamide of phthalic acid (**10**, Table 2) was obtained from a one-step reaction of the sodium amide of *p*-anisidine and diethyl phthalate in DMF.

Two methods were used for the synthesis of anthranilamides **4**. The first method started with the coupling of isatoic anhydride **11** with *p*-anisole to give amide **12** (Scheme 4).⁶ Amide **12** was acylated with the appropriate acid chlorides to provide the anthranilamides **4**. This method provided greater flexibility for B-ring variation

* Corresponding authors. E-mail: yee_ying_k@lilly.com and wiley_michael_r@lilly.com.

Scheme 3^a

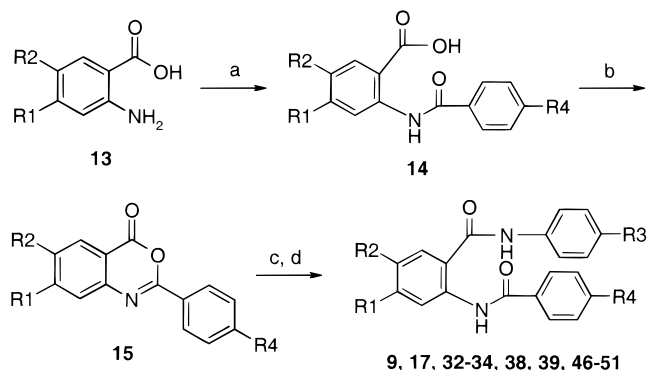
^a Reagents: (a) 4-vinylanisole, TEA, Pd(OAc)₂, 90 °C; (b) *p*-anisoyl chloride, pyridine; (c) H₂ 5% Pd/C, EtOAc.

Scheme 4^a

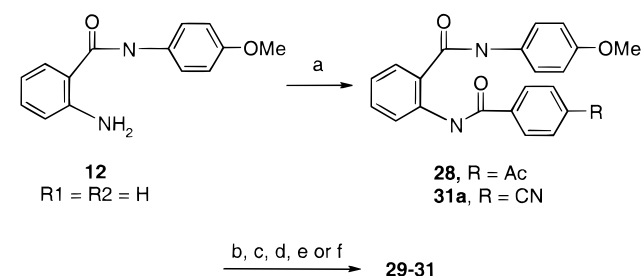
^a Reagents: (a) H₂NArR₃, PhCH₃, 80–110 °C; (b) HO₂CArR₄, pyridine, SOCl₂; or R₄PhC(O)Cl, pyridine; (c) H₂ 10% Pd/C, EtOH, EtOAc; (d) RSO₂Cl, pyridine; or succinic anhydride, pyridine.

over the second synthetic route. For the introduction of the C-ring functions, the synthesis started with nitroisatoic anhydrides. After the attachment of the A- and B-rings, functionalization of the C-ring substituent was achieved by reduction of the nitro group to an amine followed by its acylation or sulfonylation.

The second method to **4** (R₄ = *t*-Bu) utilized a nucleophilic addition of anilines to oxazinone **15** (Scheme 5).⁷ Formation of the oxazinone **15** was accomplished in two steps via acylation and cyclization with oxalyl chloride. This two-step sequence provided more pure product and greater ease of isolation of **15** over the previously described one-step procedure.⁸ Thus, anthranilic acid **13** was *N*-acylated with a slight excess of 4-*tert*-butylbenzoyl chloride to give the *N*-acylated anthranilic acid **14** plus a minor amount of the oxazinone **15**. Elevated temperature was necessary to drive the presumed initial mixed anhydride intermediate, derived from the carboxylate acylation, completely to the *N*-acylated product **14**. The mixture of *N*-acylated anthranilic acid and oxazinone was converted to oxazinone **15** with oxalyl chloride and DMF in good overall yield. The A-rings were readily introduced by heating the corresponding anilines with the oxazinone **15** in toluene at reflux to produce *N*²-acylanthranilamides **4**. This second

Scheme 5^a

^a Reagents: (a) *t*BuPhC(O)Cl, pyr, 0 °C, 50 °C; (b) ClC(O)C(O)Cl, DMF; (c) H₂NArR₃, PhCH₃, 80–110 °C; (d) H₂, 10% Pd/C, EtOH, EtOAc; (e) RSO₂Cl, pyridine; or succinic anhydride, pyridine.

Scheme 6^a

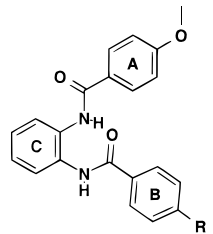
^a Reagents: (a) 4-AcPhCO₂H, SOCl₂, 80 °C; or NCPHC(O)Cl, TEA; (b) NaBH₄, MeOH, 0 °C; (c) MeMgBr, 0 °C; (d) Ni(OAc)₂, NaBH₄, 0 °C; (e) NH₂OH-HCl, NaOAc, EtOH, 80 °C, H₂, 5% Pd/C, EtOH, AcOH; (f) K₂CO₃, 30% H₂O₂, DMSO.

method was more versatile for A-ring permutations. The C-ring was functionalized as described before.

For the more functionalized B-ring moieties (**28–31**), anthranilamide **12** was acylated with 4-acetylbenzoyl chloride to afford **28** (Scheme 6). *N*-Acylanthranilamide **28** was transformed into **29** and **30** by sodium borohydride reduction and methyl Grignard addition, respectively. Compound **31** was accessed via cyano intermediate **31a**. *N*-Acylation of anthranilamide **12** with 4-cyanobenzoyl chloride provided **31a** which was hydrolyzed with hydrogen peroxide to afford carboxamide **31**.

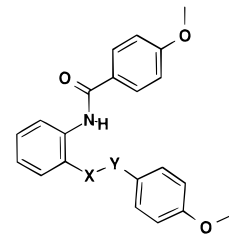
Results and Discussion

Alternative linkers to the 1,2-diamides in **1** were explored to determine the conformational and structural requirements for activity. In theory new linkers could enhance affinity in two ways: either directly, through improved interactions with the enzyme, or indirectly, by facilitating the optimal placement of the A and B aryl rings in the S1 and S4 regions of the hfxA active site.⁹ To investigate the importance of preorganization of A- and B-rings on activity, compounds containing both flexible and conformationally constrained linkers were synthesized.^{9,10} As the data in Table 2 indicate, compounds containing the flexible ether or ethyl linkers (**5**, **6**, and **8**) displayed very weak activity or inactivity. The *trans*-olefin **7**, which enforces geometry similar to the amide linker, produced a 30-fold decrease in activity relative to **1**. Likewise the phthalamide derivative **10**, in which the orientations of both of the amide linkers are reversed (retroamides), sustained an 11-fold de-

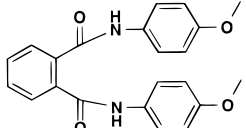
Table 1. Activity of 1,2-Dibenzamidobenzenes


compd	R	fXa K_{ass}^a ($\times 10^6$ L/mol)
1	OMe	1.3 ^b
2	tBu	7.3 ^b
3	NMe ₂	18.7 ^b

^a K_{ass} is approximately equal to $1/K_i$ (see explanatory material in Experimental Section). ^b Results reported in ref 4.

Table 2. Alternative Amide Linkers


compd	X	Y	fXa K_{ass}^a ($\times 10^6$ L/mol)
5	O	CH ₂	0.01
6	CH ₂	O	0.03
7	tCH=CH		0.03
8	CH ₂	CH ₂	<0.001
9	C(O)	NH	1.2 ^b
10			0.07

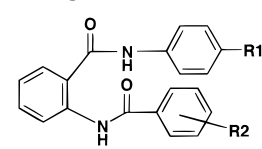


^a K_{ass} is approximately equal to $1/K_i$ (see explanatory material in Experimental Section). Each value represents the average of three separate experiments with a deviation of less than 15%.

^b Three determinations.

crease in affinity compared to **1**. Of the conformationally constrained analogues **7**, **9**, and **10**, only the anthranilamide **9** (K_{ass} of 0.81×10^6 L/mol) showed similar affinity for hfXa relative to the 1,2-dibenzamidobenzene **1**. These results demonstrate that both the rigidity of the linker and the orientation of hydrogen bond donor or acceptor groups are important for obtaining optimal activity.

The relative activity of compounds **1**, **9**, and **10** illustrates that the position of only one of the two amide linkers in **1** can be reversed without compromising enzyme affinity. To determine the relative sensitivity of each of two amide linkers (A-ring vs B-ring) to inversion, the *tert*-butylphenyl derivatives **16** and **17** (Table 3) were synthesized. As reported in our previous paper, the *tert*-butylphenyl group nicely complements the size and shape of the hydrophobic S4 site on hfXa.⁴ On the other hand, the *tert*-butylphenyl group is much too large to fit into the S1 binding site. Therefore, assuming the *p*-*tert*-butylphenyl group occupies the S4 binding site and the *p*-methoxyphenyl group binds to the S1 site in each molecule, compound **16** tests the sensitivity of the A-ring linker to inversion and com-

Table 3. Effect of B-Ring Substituents


compd	R1	R2	fXa K_{ass}^a ($\times 10^6$ L/mol)	n
16	OMe	4-tBu	4.7	5
17	tBu	4-OMe	0.03	2
18	OMe	4-Me	1.8	2
19	OMe	4-OEt	1.0	2
20	OMe	4-iPr	7.0	2
21	OMe	4-NMe ₂	20.1	3
22	OMe	4-Cl	0.27	2
23	OMe	4-CF ₃	0.09	2
24	OMe	3-Me	0.03	2
25	OMe	3-Cl	0.03	2
26	OMe	3-NMe ₂	0.09	2
27	OMe	3,4-Cl ₂	0.01	2
28	OMe	C(O)Me	0.45	1
29	OMe	CH(OH)Me	0.40	1
30	OMe	C(OH)Me ₂	0.48	1
31	OMe	C(O)NH ₂	1.12	3

^a K_{ass} is approximately equal to $1/K_i$ (see explanatory material in Experimental Section). Each value represents the average of three separate experiments with a deviation of less than 15%.

pound **17** tests the sensitivity of the B-ring linker to inversion. The hfXa affinity of **16** and **17** (Table 3) suggests that inversion of the A-ring linker is well-tolerated while inversion of the B-ring linker is detrimental to affinity for hfXa. In compound **16**, which has the A-ring linker inverted and the *tert*-butyl group introduced in the B-ring, the activity increases 4-fold relative to **9**. Compound **16** is also comparable in enzyme affinity with compound **2**, the corresponding 1,2-dibenzoylaminobenzene derivative. On the other hand, compound **17**, in which the amide connecting the central ring to the S4 binding element is inverted, sustains a 40-fold loss in activity relative to **9** and is 200-fold less active than compound **2**.

To help rationalize the possible structural details associated with the observed preference for A-ring amide inversion relative to B-ring amide inversion, molecular modeling studies were performed. hfXa active site complexes of the *p*-*tert*-butylphenyl derivatives **2** (1,2-dibenzamidobenzene), **16** (A-chain retroamide), and **17** (B-chain retroamide) were constructed and refined as described in the Experimental Section. Shown in Figure 1 is an energy-minimized molecular model for the A-chain retroamide analogue **16** in the hfXa active site. Figure 2 provides a comparison of the energy-minimized models of all three compounds: the A-chain retroamide **16** (green), the B-chain retroamide **17** (right side, orange), and the 1,2-dibenzamidobenzene **2** (left side, purple). From Figures 1 and 2 it is clear that the proposed overall binding mode for each compound is generally similar. This binding mode has been described in detail elsewhere for the 1,2-dibenzamidobenzenes related to compounds **1**–**3**.⁴ For the anthranilamides considered in the current study, the major differences in the binding mode reside in the arrangement of the two amide groups. This gives rise to differences in the possible hydrogen-bonding interactions between the ligand and the residues in the hfXa active site. Figure 1 suggests that in **16** there is an intramolecular hydrogen bond between the A-chain carbonyl oxygen

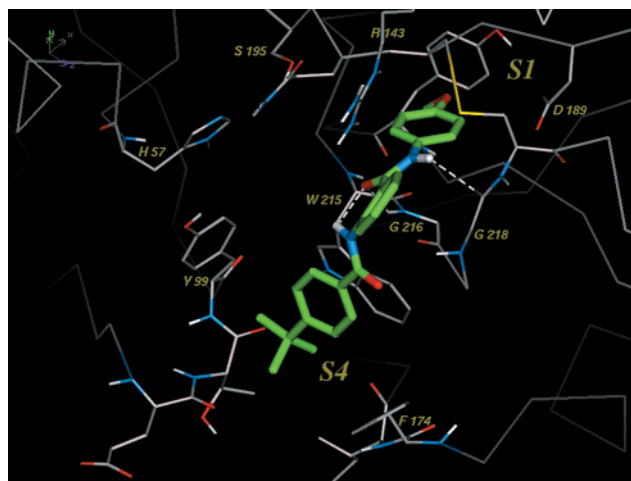


Figure 1. Proposed energy-minimized binding model of the A-chain retroamide compound **16** complexed with the active site of fXa. The orientation is such that Asp189 appears in the upper right-hand corner, Ser195 near the top central, and Glu97 in the lower left-hand corner. Hydrogen bonds between **16** and the active site for this energy-minimized structure are shown as dashed lines. All aliphatic hydrogens and waters have been removed for clarity.

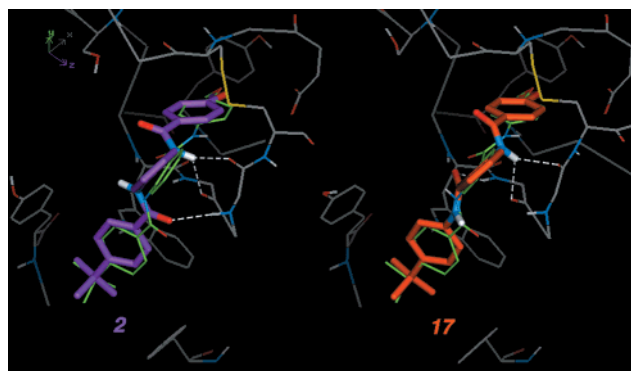


Figure 2. Proposed energy-minimized binding models of the 1,2-dibenzamidobenzene **2** (left side, purple) and the B-chain retroamide **17** (right side, orange) complexed with the active site of fXa. Included for comparison in each is the ligand from the equivalently processed complex of the A-chain retroamide **16** (green). The orientation and display features are the same as in Figure 1.

and the B-chain amide hydrogen, giving the ligand a stable conformation that incorporates a pseudo-six-membered ring. As a result, the A-chain amide hydrogen can only hydrogen bond to the carbonyl oxygen of Gly218, and the B-chain carbonyl oxygen is at too great a distance (2.7 Å) to interact with the amide of Gly218. However, inversion of the A-chain allows the amide carbonyl to form a hydrogen bond with the amide of Gly216. As a result of this interaction, the A-ring in compound **16** appears to bind slightly deeper into the S1 pocket when compared to the 1,2-dibenzamidobenzene derivative **2** (Figure 2, purple). A comparison of the A-chain retroamide **16** to the B-chain retroamide **17** (Figure 2, orange) reveals that, for the latter, the hydrogen bonds involving the A-chain are equivalent to what is found for the dibenzamidobenzene **2** and the B-chain carbonyl forms a hydrogen bond with the amide of Gly216. However, to acquire this binding mode **17** must take on a relatively high-energy conformation that places the two carbonyl groups in close proximity. A

Table 4. Effect of A-Ring Substitution

compd	R	fXa K_{ass}^a ($\times 10^6$ L/mol)	<i>n</i>
16	OMe	4.7	5
32	H	0.46	3
33	Me	3.4	2
34	Et	0.001	3
35	CF ₃	0.001	1
36	OCF ₃	<0.001	1
37	F	0.11	1
38	Cl	0.49	3
39	Br	0.22	1

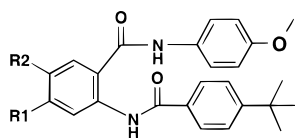
^a K_{ass} is approximately equal to $1/K_i$ (see explanatory material in Experimental Section). Each value represents the average of three separate experiments with a deviation of less than 15%.

more reasonable conformation for **17** would be similar to that illustrated for **16**, in which an internal hydrogen bond is formed between the A- and B-chains (7 kcal/mol lower in energy, CHARMM force field). However, this more stable conformation for **17** does not allow the H-bond donors and acceptors on the ligand to be placed in an orientation to reasonably bind to the protein.

In view of the results from compounds **9** and **16**, three regions of the anthranilamide may be considered for independent optimization. Results from the B-ring modification are summarized in Table 3. Consistent with the 1,2-dibenzamidobenzene series,⁴ increasing the size of the 4-substituent on the B-ring (compounds **18**–**21**) can provide a significant increase in affinity for hfXa. While the 4-*tert*-butyl (**16**) and 4-isopropyl (**20**) analogues improve affinity by 6–9-fold, the 4-dimethyl-amino group (**21**) provided the greatest enhancement in activity of 25-fold relative to the methoxy derivative **9**. Placing selected electron-withdrawing groups in the 4-position (**22** and **23**) tends to display a detrimental effect on hfXa affinity, as does the introduction of selected substituents at the 3-position of the B-ring (**24**–**27**).

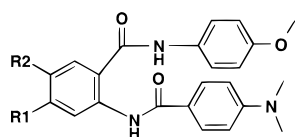
The enhanced affinity observed with compounds **20** and **21** led us to examine B-ring moieties which mimic the size and shape of the isopropyl group and are also capable of participating in hydrogen-bonding or ionic interactions. Compounds **28**–**31** containing a variety of hydrogen bond-donating and -accepting groups at the 4-position all have weaker affinity than **20** and **21**.

Table 4 shows the results of SAR studies on the S1 binding element and illustrates the sensitivity of this binding site to structural variation. In this series, the 4-*tert*-butyl group was used as the B-ring substituent to ensure that no binding of the B-ring into the S1 pocket could obscure the results. Comparing the results for compound **32** (R = H) with compounds **33** (R = Me) and **16** (R = MeO) demonstrates that in this series the 4-methyl and 4-methoxy groups contribute 7–10-fold to the enzyme affinity. However, even subtle changes in the size and shape of the S1 binding elements can have a significant detrimental effect on activity. The 5000-fold loss in activity suffered by the 4-ethyl derivative **34** relative to **16** demonstrates that 4-substituents must be able to achieve a conformation coplanar with the A-ring in order to maintain reasonable affinity. Other

Table 5. Effect of C-Ring Substituents

compd	R1	R2	fXa K_{ass}^a ($\times 10^6$ L/mol)	<i>n</i>
40	NO ₂	H	0.08	1
41	NH ₂	H	6.3	3
42	NHSO ₂ Me	H	3.9	2
43	NHSO ₂ Ph	H	0.62	2
44	NHAc	H	2.2	3
45	NHC(O)CH ₂ CH ₂ CO ₂ H	H	9.6	3
46	H	NO ₂	2.1	4
47	H	NH ₂	2.5	2
48	H	NHSO ₂ Me	13.5	3
49	H	NHSO ₂ Ph	4.9	3
50	H	NHAc	0.04	2
51	H	NHC(O)CH ₂ CH ₂ CO ₂ H	0.15	3

^a K_{ass} is approximately equal to $1/K_i$ (see explanatory material in Experimental Section). Each value represents the average of three separate experiments with a deviation of less than 15%.

Table 6. Additive Effect of B- and C-Ring Substituents

compd	R1	R2	fXa K_{ass}^a ($\times 10^6$ L/mol)	<i>n</i>
52	NH ₂	H	22.7	3
53	H	NH ₂	7.0	2
54	MeSO ₂ NH	H	8.0	2
55	H	MeSO ₂ NH	57.9 ^b	3
56	HO ₂ CCH ₂ CH ₂ C(O)NH	H	9.6	2
57	H	HO ₂ CCH ₂ CH ₂ C(O)NH	0.4	2

^a K_{ass} is approximately equal to $1/K_i$ (see explanatory material in Experimental Section). Each value represents the average of three separate experiments with a deviation of less than 15%. ^b K_i was determined to be 11.5 ± 2.13 nM ($n = 3$) (see Experimental Section).

subtle increases in the size of the 4-substituent also resulted in significant losses in activity. The 4-trifluoromethyl derivative **35** and 4-trifluoromethoxy **36** were inactive. The 4-halo analogues **37–39** resulted in 10–44-fold drops in affinity when compared to **16**.

The SAR of the retroamides **4** directly parallels that of the 1,2-dibenzamidobenzenes as illustrated by the relative affinity of **9**, **16**, and **21** with **1**, **2**, and **3**, respectively. This correspondence between the two series strongly suggests that they both bind to the hfXa in a similar fashion as indicated by the modeling studies.

The C-ring substituent effects were explored by using an amino substituent to introduce a variety of functional groups (Table 5). In the 4-substituted series (**40–45**), the amino group (**41**) has a minimal effect on affinity compared to **16**. While the methanesulfamoyl derivative (**42**) was essentially equivalent to **16**, the succinoylamino group (**45**) produced a 2-fold increase in hfXa affinity. The SAR in the 5-substituted series diverged from that of the 4-substituted congeners. In this series, the 5-methanesulfamoyl derivative (**48**) was the most potent C-ring substituent producing nearly a 3-fold increase in activity. This modest improvement in activity was expected since modeling studies showed that the 4- and 5-positions of the C-ring lie outside of the hfXa binding pocket. Unlike the 4-substituted derivative

which had a positive effect, the 5-succinoylamino (**51**) decreased affinity by 31-fold.

Results from incorporation of groups, which were beneficial in the C-ring SAR, into the *p*-dimethylamino B-ring series are shown in Table 6. While the 4-amino derivative **52** maintained the activity of the unsubstituted parent compound **21**, both the 4-methanesulfamoyl (**54**) and 4-succinoylamino (**56**) derivatives decreased affinity by about one-half. In the 5-substituted series, the succinoylamino group (**57**) caused a 50-fold loss in hfXa affinity. In contrast, the 5-methanesulfamoyl group (**55**) enhanced affinity by 3-fold over **21**. Compound **55** is the most potent analogue within this series with a K_{ass} for human fXa of 58×10^6 L/mol. In addition, the K_i for **55** was determined by Dixon plots and was found to be 11.5 ± 2.13 nM ($n = 3$) with classical competitive inhibition curves. Thus, the C-ring SAR in the *p*-dimethylamino B-ring series closely parallels that of the *tert*-butyl B-ring series.

Conclusion

Investigation of alternative linking groups relative to 1,2-dibenzamidobenzenes led to the discovery of N²-aroylanthranilamides **4** with enhanced activity. Molecular modeling studies suggested that N²-aroylanthranilamides **4** having an inverted A-chain bind to hfXa in a similar mode as the 1,2-dibenzamidobenzenes. On the

other hand, anthranilamides having an inverted B-chain had considerably diminished enzyme affinity.

Experimental Section

All reactions were run under an atmosphere of dry nitrogen unless noted. All solvents and reagents were used as acquired from commercial sources without purification. Nuclear magnetic resonance spectra were recorded at 300 MHz on a GE QE-300 spectrophotometer in the solvent indicated. Chemical shifts are reported in parts per million relative to tetramethylsilane. Infrared spectra were recorded on a Nicolet DX10 FT-IR spectrometer. Melting points were recorded on a Thomas-Hoover melting point apparatus and are uncorrected. Mass spectra were recorded on the following instruments, using the stated ionization methods: VG Analytical 70SE mass spectrometer, field-desorption (FD); VG Analytical ZAB2-SE instrument, fast atom bombardment (FAB); Sciex API 100 mass spectrometer, electrospray ionization (ESI). Elemental analyses were performed by the Physical Chemistry Department at Lilly Research Laboratories on a Control Equipment Corp. 440 elemental analyzer and are within 0.4% of theory unless otherwise noted.

Experimental conditions for key compounds **9**, **16**, **18**, **21**, **29–32**, **36**, **37**, **40–42**, **46–48**, and **52–55** are described in detail below. Preparations for related compounds using analogous procedures are in the Supporting Information.

Materials. hfXa and human thrombin were purchased from Enzyme Research Laboratories (South Bend, IN). Chromogenic *p*-nitroanilide peptide protease substrates were purchased from Midwest Biotech (Fishers, IN): Bz-Ile-Glu-Gly-Arg-pNA (for hfXa) and Bz-Phe-Val-Arg-pNA (for thrombin).

Molecular Modeling. The protein structure coordinate set used in this investigation was the hfXa X-ray structure of Padmanabhan et al.¹⁴ (Brookhaven PDB file 1hcg). The computational construction of ligands and protein–ligand complexes and the graphical analysis of results were performed with QUANTA, version 96.¹⁵ Energy minimization was performed using CHARMM, version 23.2.^{15,16} Details of the initial computational preparation of the hfXa X-ray protein structure as well as the derivation of the bisamide phenyl ligand template have been described by Herron et al.⁴ This solvated, all hydrogen, initial protein system coordinate set was used as the starting point for all protein–ligand complexes modeled. Energy evaluation and minimization were done using the same nonbond settings, algorithm criteria, and constraint regime as previously reported.⁴ The 3D starting structures for analogues **2**, **16** (A-chain retroamide), and **17** (B-chain retroamide) were constructed by modifying the 1,2-dibenzamidobenzene template. Modifications for each were made using the 3D Editor, maintaining the original conformation and also position in space. Default atom types and charges were assigned, the latter smoothed over all C and nonpolar H atoms to give a total sum of 0.0. Each analogue was then processed by reinserting into the active site of the fully solvated hfXa protein starting structure, deleting waters having an oxygen within 2.0 Å of a ligand atom, and then refining the complex by constrained energy minimization. The final energy-minimized structures are shown in Figure 1 (**16**, green) and Figure 2 (**2**, purple; **17**, orange). In both figures all aliphatic hydrogens and waters have been removed for clarity.

Binding Affinity for hfXa. The binding affinities for hfXa were measured as apparent association constants (K_{ass}) derived from protease inhibition kinetics as described previously.^{12,13} The apparent K_{ass} values were obtained in a high-volume protocol using automated dilutions of inhibitors ($n = 3$ for each of four to eight inhibitor concentrations) into 96-well plates and chromogenic substrate hydrolysis rates determined at 405 nm using a Thermomax plate reader from Molecular Devices (San Francisco, CA). For the assay protocol, 25 μL inhibitor test solution (in MeOH) was added to 50 μL buffer (0.06 M tris, 0.3 M NaCl, pH 7.4) followed by 25 μL hfXa (32 nM in 0.03 M tris, 0.15 M NaCl, 1 mg/mL HSA). Finally, 150 μL substrate (0.3 mM in water) was added within 2 min to start hydrolysis. The final fXa concentration was 3.2 nM. Free [fXa]

and bound [fXa] were determined from linear standard curves on the same plate by use of SoftmaxPro software for each inhibitor concentration and apparent K_{ass} calculated for each inhibitor concentration which produced hydrolysis inhibition between 20% and 80% of the control (3.2 nM fXa): apparent $K_{\text{ass}} = [\text{E}]/[\text{E}_\text{f}][\text{I}_\text{f}] = [\text{E}_\text{b}]/[\text{E}_\text{f}][\text{I}^\circ - \text{I}_\text{b}]$. This method allows affinity determinations for tight binding inhibitors as well as for weak binding enzyme inhibitors and has generated a large protease inhibitor SAR database.¹³ This system of affinity measurement was designed to (1) validly assess a very large number of protease inhibitor samples and (2) determine affinity with tight binding inhibitors where classical K_i methods fail.^{17,18} Algebraic solutions for the equation $K_{\text{ass}} = [\text{E}]/[\text{E}_\text{f}][\text{I}_\text{f}] = [\text{E}_\text{b}]/[\text{E}_\text{f}][\text{I}^\circ - \text{I}_\text{b}]$ account for the free and bound inhibitor concentrations. Alternatively, the whole data set can be graphically analyzed as a linearized solution to the same K_{ass} equation: $\text{I}^\circ/(1 - a) = [1/\text{apparent } K_{\text{ass}}(a)] + \text{E}^\circ$, where a = fraction of free enzyme.¹³ This equation was also derived by Henderson¹⁷ and Bieth¹⁸ for study of tight binding inhibitors, where classical methods fail to account for bound inhibitor concentrations.

The application of this method has facilitated the accumulation of a large database of apparent K_{ass} values (obtained at a single appropriate substrate concentration with each protease of interest) which are self-consistent for each protease.^{12,13} Apparent K_{ass} values can be corrected by determining the effect of substrate concentration (apparent $K_{\text{ass}} = 1/\text{apparent } K_i$; corrected $K_{\text{ass}} = 1/K_i$).^{13,17,18} The variability of mean apparent K_{ass} values determined at the single substrate concentration was $\pm 15\%$. The assay system K_m was measured as 0.347 ± 0.031 mM ($n = 4$), and V_{max} was 13.11 ± 0.76 $\mu\text{M}/\text{min}$. For classical K_i determinations Dixon plots were generated with the same protocol using four substrate concentrations (0.112, 0.224, 0.448, 0.896 mM), and the type of inhibition was confirmed with Lineweaver–Burke graphs.

Preparation of *N*-(4-Methoxyphenyl)-2-(4-methoxybenzamido)benzamide (9). (a) **Methyl 2-(4-Methoxybenzoyl)aminobenzoate (9a).** To a solution of methyl 2-aminobenzoate (6.46 mL, 50 mmol) in methylene chloride (150 mL) at 0 °C was added triethylamine (7.02 mL, 50 mmol) followed by *p*-anisoyl chloride (8.55 g, 50 mmol). The reaction mixture was warmed to room temperature (rt) and stirred for 16 h. The reaction was shaken with cold dil HCl (200 mL) followed by satd K_2CO_3 (200 mL). The organic layer was dried (MgSO_4) and concentrated in vacuo. The residue was crystallized with hexane to give **9a** as a solid (12.0 g, 84%): ^1H NMR (DMSO- d_6) δ 3.86 (s, 3H), 3.90 (s, 3H), 7.14 (d, 2H), 7.23 (t, 1H), 7.96 (d, 2H), 8.02 (d, 1H), 8.60 (d, 1H), 11.56 (s, 1H); MS-FD m/e 285 (M^+). Anal. ($\text{C}_{16}\text{H}_{15}\text{NO}_4$) C, H, N.

(b) **2-((4-Methoxybenzoyl)amino)benzoic Acid (9b).** To a mixture of **9a** (2.0 g, 7.01 mmol) and MeOH (50 mL) was added 5 N NaOH (10 mL, 50 mmol) and stirred for 4 h. Most of the solvent was removed in vacuo and the mixture was partitioned between water (100 mL) and EtOAc (100 mL). The aqueous layer was acidified with dil HCl and extracted with EtOAc (150 mL). The organic layer was dried (MgSO_4) and concentrated in vacuo. The residue was crystallized from methylene chloride and hexane to give **9b** as a solid (1.56 g, 82%): ^1H NMR (DMSO- d_6) δ 3.85 (s, 3H), 7.12 (d, 2H), 7.19 (t, 1H), 7.65 (t, 1H), 7.92 (d, 2H), 8.05 (d, 1H), 8.70 (d, 1H), 12.13 (s, 1H), 13.76 (s, 1H); MS-FD m/e 271 (M^+). Anal. ($\text{C}_{15}\text{H}_{13}\text{NO}_4$) C, H, N.

(c) **2-(4-Methoxyphenyl)-4H-3,1-benzoxazin-4-one (9c).** To a 0 °C mixture of **9b** (1.36 g, 5.0 mmol), methylene chloride (75 mL), and DMF (2 drops) was added oxalyl chloride (0.50 mL, 5.5 mmol). After 30 min, the reaction was warmed to rt and stirred for 1 h. The solvent was removed in vacuo at 35 °C to give a solid. The solid was dissolved in methylene chloride (50 mL) and treated with 0.94 mL (6.66 mmol) triethylamine at rt. After 16 h the reaction mixture was diluted with 50 mL methylene chloride and shaken with 200 mL 5 N HCl and 200 mL satd K_2CO_3 . Organic layer was dried (MgSO_4) and concentrated in vacuo. The product crystallized from CH_2Cl_2 and hexanes to give **9c** (0.698 g, 55%): ^1H NMR (DMSO- d_6) δ 3.88

(s, 3H), 7.14 (d, 2H), 7.60 (t, 1H), 7.68 (d, 1H), 7.94 (t, 1H), 8.15 (d, 1H), 8.18 (d, 2H); MS-FD *m/e* 253 (M⁺). Anal. for C₁₅H₁₁NO₃: Calcd: C, 71.14; H, 4.38; N, 5.53. Found: C, 71.08; H, 4.58; N, 5.12.

(d) *N*-(4-Methoxyphenyl)-2-(4-methoxybenzamido)-benzamide (9). A mixture of **9c** (0.253 g, 1 mmol) ethanol (25 mL), and *p*-anisidine (0.123 g, 1 mmol) was refluxed for 4 h. After cooling, the product was crystallized and filtered with ethanol wash to give **9** as a solid (0.106 g, 28%): ¹H NMR (DMSO-*d*₆) δ 3.73 (s, 3H), 3.81 (s, 3H), 6.93 (d, 2H), 7.09 (d, 2H), 7.23 (t, 1H), 7.23 (t, 1H), 7.57 (t, 1H), 7.58 (d, 2H), 7.85 (d, 2H), 7.90 (d, 1H), 8.52 (d, 1H), 10.42 (s, 1H), 11.81 (s, 1H); MS-FD *m/e* 376 (M⁺). Anal. (C₂₂H₂₀N₂O₄) C, H, N.

Preparation of 2-(4-*tert*-Butylbenzoylamino)-*N*-(4-methoxyphenyl)benzamide (16). **(a) 2-Amino-*N*-(4-methoxyphenyl)benzamide (16a).** A mixture of isatoic anhydride (4.9 g, 30 mmol), *p*-anisidine (3.7 g, 30 mmol) in toluene (60 mL) was heated to reflux for 5 h.⁶ After cooling, the supernatant was decanted and the solid was suspended in methylene chloride (500 mL). The resulting suspension was filtered. The filtrate was combined with the supernatant from above, partially concentrated, diluted with hexane, and decolorized with charcoal. The solution was concentrated and crystallized to yield **16a** as a white solid (5.3 g, 73%): mp 116–117 °C; ¹H NMR (300 MHz, DMSO-*d*₆) δ 3.81 (s, 3H), 6.72 (m, 2H), 6.91 (d, *J* = 9.0 Hz, 2H), 7.26 (m, 1H), 7.45 (d, *J* = 6.8 Hz, 1H), 7.46 (d, *J* = 9.0 Hz, 2H); MS-FD *m/e* 242 (M⁺). Anal. (C₁₄H₁₄N₂O₂) C, H, N.

(b) 2-(4-*tert*-Butylbenzoylamino)-*N*-(4-methoxyphenyl)-benzamide (16). To a 0 °C mixture of **16a** (728 mg, 3.0 mmol), pyridine (0.39 mL, 4.5 mmol), and CH₂Cl₂ (30 mL) was added *tert*-butylbenzoyl chloride (0.57 mL, 3.06 mmol). The reaction was warmed to rt and stirred for 2 h. The reaction was partially concentrated, stirred vigorously with 1 N HCl (20 mL) and filtered to yield **11** as a white solid (809 mg, 67%): mp 208–210 °C; ¹H NMR (300 MHz, DMSO-*d*₆) δ 1.31 (s, 9H), 3.76 (s, 3H), 6.96 (d, *J* = 9.0 Hz, 2H), 7.27 (m, 1H), 7.60 (m, 5H), 7.87 (d, *J* = 8.3 Hz, 2H), 7.94 (d, *J* = 8.0 Hz, 1H), 8.57 (d, *J* = 8.0 Hz, 1H), 10.45 (s, 1H), 11.90 (s, 1H); MS-FD *m/e* 402 (M⁺). Anal. (C₂₅H₂₆N₂O₃) C, H, N.

2-(4-Methylbenzoylamino)-*N*-(4-methoxyphenyl)benzamide (18). Using a procedure described for **16**, 4-methylbenzoyl chloride yielded **18** (64%): ¹H NMR (300 MHz, DMSO-*d*₆) δ 2.38 (s, 3H), 3.75 (s, 3H), 6.95 (d, *J* = 9.2 Hz, 2H), 7.26 (m, 1H), 7.37 (d, *J* = 8.1 Hz, 2H), 7.60 (m, 3H), 7.81 (d, *J* = 8.1 Hz, 2H), 7.93 (d, *J* = 7.7 Hz, 1H), 8.54 (d, *J* = 8.4 Hz, 1H), 10.43 (s, 1H), 11.86 (s, 1H); FIA-MS *m/e* 359.2 (M – 1). Anal. (C₂₂H₂₀N₂O₃) C, H, N.

2-(4-Dimethylaminobenzoylamino)-4-amino-*N*-(4-methoxyphenyl)benzamide (21). To a mixture of 4-dimethylaminobenzoic acid (10 g, 60.5 mmol) and CH₂Cl₂ (400 mL) was added thionyl chloride (6.6 mL, 90.5 mmol). The reaction was refluxed for 3 h and concentrated in vacuo to give 4-dimethylaminobenzoyl chloride (11.11 g, quant). 4-Dimethylaminobenzoyl chloride (377 mg, 2.05 mmol) was added to a solution of 2-amino-*N*-(4-methoxyphenyl)benzamide (304 mg, 1.25 mmol), pyridine (0.15 mL, 1.85 mmol), DMAP (159 mg, 1.30 mmol) and CH₂Cl₂ (15 mL). After stirring for 14 h, the reaction was diluted with CH₂Cl₂ (75 mL) and washed with satd Na₂CO₃ (2 × 10 mL). The organic layer was dried (Na₂SO₄) and concentrated. The residue was chromatographed on (CH₂Cl₂ to 5% EtOAc/CH₂Cl₂) to yield **21** as a white solid (444 mg, 91%): ¹H NMR (300 MHz, DMSO-*d*₆) δ 2.96 (s, 6H), 3.72 (s, 3H), 6.76 (d, *J* = 9.0 Hz, 2H), 6.92 (d, *J* = 8.7 Hz, 2H), 7.17 (m, 1H), 7.59–7.54 (m, 3H), 7.72 (d, *J* = 9.0 Hz, 2H), 7.88 (d, *J* = 7.5 Hz, 1H), 8.57 (d, *J* = 8.1 Hz, 1H), 10.39 (s, 1H), 11.74 (s, 1H); MS-ES *m/e* 390.2 (M + H). Anal. (C₂₃H₂₃N₃O₃) C, H, N.

2-[4-(1-Hydroxyethyl)benzoylamino]-*N*-(4-methoxyphenyl)benzamide (29). To a solution of **28** (101 mg, 0.260 mmol) in methanol (5 mL) cooled to 0 °C was added sodium borohydride (17 mg, 0.46 mmol). After 20 min, the reaction mixture was quenched with saturated aqueous ammonium chloride solution (1 mL), diluted with methylene chloride (30

mL), and washed with water. The organic layer was dried (MgSO₄), filtered, and concentrated in vacuo. The residue was chromatographed (silica gel, 25% ethyl acetate/75% hexanes to 50% ethyl acetate/50% hexanes) to give **29** (85 mg, 84%): ¹H NMR (CDCl₃) δ 1.52 (d, *J* = 7.5 Hz, 3H), 3.83 (s, 3H), 4.97 (q, *J* = 7.8 Hz, 1H), 6.95 (d, *J* = 10.5 Hz, 2H), 7.07 (t, *J* = 9.0 Hz, 1H), 7.51 (m, 6H), 7.99 (d, *J* = 9.9 Hz, 2H), 8.17 (s, 1H), 8.72 (d, *J* = 9.9 Hz, 1H), 11.79 (s, 1H); MS-FD *m/e* 390 (M⁺). Anal. (C₂₃H₂₂N₂O₄·0.25H₂O) C, H, N.

2-[4-[2-(2-Hydroxypropyl)]benzoylamino]-*N*-(4-methoxyphenyl)benzamide (30). To a solution of **28** (161 mg, 0.410 mmol) in tetrahydrofuran (10 mL) cooled to 0 °C was added 3 M methylmagnesium bromide in diethyl ether (0.2 mL, 0.6 mmol). After 1 h, the reaction mixture was quenched with saturated aqueous ammonium chloride solution (2 mL), diluted with ether, and washed with water. The organic layer was dried (MgSO₄), filtered, and concentrated in vacuo. The residue was chromatographed (silica gel, 15% ethyl acetate/85% hexanes to 35% ethyl acetate/65% hexanes) to give **30** (24 mg, 14%): ¹H NMR (CDCl₃) δ 1.64 (d, *J* = 9.3 Hz, 6H), 3.88 (s, 3H), 6.99 (d, *J* = 3.7 Hz, 2H), 7.13 (t, *J* = 8.4 Hz, 1H), 7.55–7.67 (m, 6H), 8.02 (d, *J* = 8.4 Hz, 2H), 8.17 (s, 1H), 8.78 (d, *J* = 8.4 Hz, 1H); MS-FD *m/e* 404 (M⁺); HRMS (C₂₄H₂₄N₂O₄-Na) theoretical 427.1634, found 427.1634 (M + Na).

Preparation of *N*-(4-Methoxyphenyl)-2-[4-(aminocarbonyl)benzamido]benzamide (31). **(a) *N*-(4-Methoxyphenyl)-2-(4-cyanobenzamido)benzamide (31a).** Using a procedure described in **16b**, *N*-(4-methoxyphenyl)-2-aminobenzamide and 4-cyanobenzoyl chloride yielded **31a** (76%): ¹H NMR (DMSO-*d*₆) δ 3.71 (s, 3H), 6.91 (d, 2H), 7.28 (t, 1H), 7.56 (d, 2H), 7.59 (t, 1H), 7.90 (d, 2H), 8.02 (s, 4H), 8.39 (d, 1H), 10.43 (s, 1H), 11.91 (s, 1H); MS-ES *m/e* 372 (M + H). Anal. (C₂₂H₁₇N₃O₃) C, H, N.

(b) *N*-(4-Methoxyphenyl)-2-[4-(aminocarbonyl)benzamido]benzamide (31). To a mixture of **31a** (0.5 g, 1.35 mmol), DMSO (10 mL), and K₂CO₃ (0.5 g, 3.62 mmol) was added 30% H₂O₂ (1 mL, 8.82 mmol). After stirring for 1 h, the reaction mixture was diluted with water (100 mL) and the precipitate was filtered and dried to give **31** (0.45 g, 86%): ¹H NMR (DMSO-*d*₆) δ 3.75 (s, 3H), 6.91 (d, 2H), 7.26 (t, 1H), 7.58 (d, 2H), 7.59 (t, 1H), 7.91 (d, 1H), 7.94 (d, 2H), 7.99 (d, 1H), 8.03 (s, 1H), 8.09 (s, 1H), 8.50 (d, 1H), 10.43 (s, 1H), 11.90 (s, 1H); MS-ES *m/e* 390 (M + H). Anal. (C₂₂H₁₉N₃O₃) C, H, N.

Preparation of 2-[(4-*tert*-Butylbenzoyl)amino]-*N*-phenylbenzamide (32). **(a) 2-(4-*tert*-Butylphenyl)-4H-3,1-benzoxazin-4-one (32a).** To a stirred solution of anthranilic acid (34.3 g, 250 mmol) in pyridine (400 mL) was added 4-*tert*-butylbenzoyl chloride (94 mL, 502 mmol) dropwise. The reaction was for 12 h and poured onto ice and 2 N hydrochloric acid (100 mL). After partitioning, the organic layer was washed with 2 N hydrochloric acid, satd sodium chloride, satd sodium bicarbonate, water, dried (MgSO₄), and concentrated in vacuo. The residue was crystallized from ether/hexanes to give **32a** (32.1 g, 46%): ¹H NMR (DMSO-*d*₆) δ 8.26 (m, 3H), 7.83 (t, *J* = 8.7 Hz, 1H), 7.70 (d, *J* = 8.7 Hz, 1H), 7.52 (m, 3H), 1.39 (s, 9H); MS-FIA 280.2 (M⁺). Anal. (C₁₈H₁₇N₂O₂) C, H, N.

(b) 1-*N*-Phenyl-2-*N*-(4-*tert*-butylbenzoyl)anthranilamide (32). A mixture of **32a** (1.0 g, 3.6 mmol), aniline (0.33 g, 3.6 mmol) and toluene (15 mL) was refluxed for 8 h. After cooling, the reaction was added diethyl ether and filtered to **32** (120 mg, 9%): ¹H NMR (300 MHz, DMSO-*d*₆) δ 1.30 (s, 9H), 7.14 (t, *J* = 7.5 Hz, 1H), 7.27 (dt, *J* = 0.8, 7.9 Hz, 1H), 7.37 (t, *J* = 7.9 Hz, 2H), 7.59 (d, *J* = 8.7 Hz, 2H), 7.61 (m, 1H), 7.71 (d, *J* = 7.9 Hz, 2H), 7.84 (d, *J* = 8.7 Hz, 2H), 7.93 (dd, *J* = 1.1, 7.5 Hz, 1H), 8.51 (d, *J* = 7.9 Hz, 1H), 10.53 (s, 1H), 11.70 (s, 1H); MS-FD *m/e* 372. Anal. (C₂₄H₂₄N₂O₂) C, H, N.

Preparation of 2-(4-*tert*-Butylbenzoyl)amino-*N*-(4-trifluoromethoxyphenyl)benzamide (36). **(a) 2-Amino-*N*-(4-trifluoromethoxyphenyl)benzamide (36a).** To a stirring solution of 4-(trifluoromethoxy)aniline (0.34 mL, 2.5 mmol) in dichloromethane (15 mL) was added pyridine (0.6 mL, 7.5 mmol), followed by 2-nitrobenzoyl chloride (0.36 mL, 2.7 mmol). After 1 h, the solvent was removed in vacuo and the residue was partitioned between ethyl acetate and water. The

organic phase was separated and washed twice with 1 M citric acid, once with brine, twice with satd aq NaHCO₃, and again with brine. The organic phase was then dried with MgSO₄, filtered and the filtrate was concentrated. The resulting solid was then suspended in ether, sonicated, filtered and dried to give 0.67 g of a white solid.

The solid was then dissolved in THF (60 mL) and to this stirring solution (under nitrogen) was added 10% Pd/C (0.3 g). The reaction was hydrogenated overnight at atmospheric pressure and filtered. The filtrate was concentrated and the residue was dissolved in ether. The organic phase was washed with water and brine, dried (MgSO₄), and concentrated to give of **36a** as a white solid (0.43 g, 77%): ¹H NMR (300 MHz, DMSO-*d*₆) δ 6.32 (br s, 2H), 6.58 (t, *J* = 7.2 Hz, 1H), 6.75 (d, *J* = 8.3 Hz, 1H), 7.20 (t, *J* = 7.2 Hz, 1H), 7.33 (d, *J* = 8.7 Hz, 2H), 7.62 (d, *J* = 7.9 Hz, 1H), 7.82 (d, *J* = 8.7 Hz, 2H), 10.14 (s, 1H); MS-FD *m/e* 296.1. Anal. (C₁₄H₁₁N₂O₂F₃) C, H, N.

(b) **2-(4-*tert*-Butylbenzoyl)amino-*N*-(4-trifluoromethoxyphenyl)benzamide (36).** Using a procedure described in **16b**, **36a** yielded **36** as a white solid (0.207 g, 89%): ¹H NMR (300 MHz, DMSO-*d*₆) δ 1.30 (s, 9H), 7.29 (dt, *J* = 1.1, 7.5 Hz, 1H), 7.38 (d, *J* = 9.0 Hz, 2H), 7.58 (d, *J* = 8.3 Hz, 2H), 7.62 (dt, *J* = 1.1, 7.9 Hz, 1H), 7.82 (d, *J* = 9.0 Hz, 2H), 7.83 (d, *J* = 8.3 Hz, 2H), 8.47 (d, *J* = 8.3 Hz, 1H), 10.68 (s, 1H), 11.54 (s, 1H); MS-FD *m/e* 456.2. Anal. (C₂₅H₂₃N₂O₃F₃) C, H, N.

Preparation of 2-(4-*tert*-Butylbenzoyl)amino-*N*-(4-fluorophenyl)benzamide (37). (a) **1-*N*-(4-Fluorophenyl)-2-nitrobenzamide (37a).** Using a procedure described in **36a**, 4-fluoroaniline yielded **37a** (79%): ¹H NMR (300 MHz, DMSO-*d*₆) δ 7.21 (t, *J* = 9.0 Hz, 2H), 7.67 (dd, *J* = 5.3, 9.0 Hz, 2H), 7.70–7.80 (m, 3H), 7.87 (t, *J* = 7.5 Hz, 1H), 8.15 (d, *J* = 8.3 Hz, 1H), 10.71 (s, 1H); MS-FD *m/e* 260 (M⁺). Anal. (C₁₃H₉N₂O₃F) C, H, N.

(b) **2-Amino-*N*-(4-fluorophenyl)benzamide (37b).** To a stirred mixture of **37a** (4.0 g, 15.4 mmol), methanol (220 mL), tetrahydrofuran (110 mL) and nickel acetate tetrahydrate (7.7 g, 31 mmol) was added sodium borohydride (2.3 g, 62 mmol) was added in small portions. After gas evolution had ceased, the solvent was removed in vacuo. The residue was partitioned between ethyl acetate and concentrated ammonium hydroxide. The organic layer was washed with concentrated ammonium hydroxide and satd sodium chloride, dried (MgSO₄), filtered, and concentrated to give **37b** (2.86 g, 81%): ¹H NMR (300 MHz, DMSO-*d*₆) δ 6.31 (br s, 2H), 6.58 (dt, *J* = 1.1, 7.9 Hz, 1H), 6.75 (d, *J* = 7.9 Hz, 1H), 7.16 (d, *J* = 8.7 Hz, 2H), 7.15–7.25 (m, 1H), 7.60 (d, *J* = 7.9 Hz, 1H), 7.71 (dd, *J* = 5.3, 9.0 Hz, 2H), 10.02 (s, 1H); MS-FD *m/e* 230.2 (M⁺). Anal. (C₁₃H₁₁N₂OF) C, H, N.

(c) **2-(4-*tert*-Butylbenzoyl)amino-*N*-(4-fluorophenyl)benzamide (37).** Using the procedure described in **16b**, **37b** yielded **37** (1.03 g, 64%): ¹H NMR (300 MHz, DMSO-*d*₆) δ 1.31 (s, 9H), 7.22 (t, *J* = 9.0 Hz, 2H), 7.28 (t, *J* = 7.5 Hz, 1H), 7.55–7.65 (m, 3H), 7.73 (dd, *J* = 5.3, 9.0 Hz, 2H), 7.85 (d, *J* = 8.3 Hz, 2H), 7.93 (d, *J* = 7.5 Hz, 1H), 8.51 (d, *J* = 8.3 Hz, 1H), 10.57 (s, 1H), 11.69 (s, 1H); MS-FD *m/e* 230.2 (M⁺). Anal. (C₂₄H₂₃N₂O₂F) C, H, N.

Preparation of 2-(4-*tert*-Butylbenzoyl)amino-4-nitro-*N*-(4-methoxyphenyl)benzamide (40). (a) **2-Amino-4-nitro-*N*-(4-methoxyphenyl)benzamide (40a).** Using a procedure described in **16a**, 4-nitroisatoic anhydride and *p*-anisidine yielded **40a** as a greenish yellow solid (95%): mp 193–197 °C; ¹H NMR (DMSO-*d*₆) δ 3.72 (s, 3H), 6.23 (br s, 2H), 6.90 (d, 2H, *J* = 9.3 Hz), 7.33 (dd, 1H, *J* = 2.1, 8.7 Hz), 7.59 (d, *J* = 9.3 Hz, 1H), 7.59 (d, *J* = 2.1 Hz, 1H), 7.77 (d, *J* = 8.7 Hz, 2H), 10.19 (s, 1H); MS-FD *m/e* 287. Anal. (C₁₄H₁₃N₃O₄) C, H, N.

(b) **2-(4-*tert*-Butylbenzoyl)amino-4-nitro-*N*-(4-methoxyphenyl)benzamide (40).** Using a procedure described in **16b**, **40a** yielded **40** as a yellow solid (77%): mp 221 °C; ¹H NMR (300 MHz, DMSO-*d*₆) δ 1.36 (s, 9H), 3.84 (s, 3H), 6.97 (d, *J* = 9.0 Hz, 2H), 7.55 (m, 4H), 7.76 (d, *J* = 8.7 Hz, 1H), 7.87 (dd, *J* = 2.3, 8.7 Hz, 1H), 7.94 (d, *J* = 8.3 Hz, 2H), 8.66 (br s, 1H), 9.65 (d, *J* = 2.3 Hz, 1H), 11.77 (br s, 1H); MS-FD *m/e* 447 (M⁺). Anal. (C₂₅H₂₅N₃O₅) C, H, N.

2-(4-*tert*-Butylbenzoyl)amino-4-amino-*N*-(4-methoxyphenyl)benzamide (41). Using a procedure analogous to **6b**, **40** was hydrogenated in a mixture of ethyl acetate, ethanol, and glacial acetic acid to yield **41** (61%): mp 137–140 °C; ¹H NMR (300 MHz, DMSO-*d*₆) δ 1.31 (s, 9H), 3.75 (s, 3H), 5.98 (br s, 2H), 6.34 (dd, *J* = 2.3, 9.0 Hz, 1H), 6.92 (d, *J* = 9.0 Hz, 2H), 7.54 (d, *J* = 9.0 Hz, 2H), 7.58 (d, *J* = 8.3 Hz, 2H), 7.73 (d, *J* = 9.0 Hz, 1H), 7.84 (d, *J* = 8.3 Hz, 2H), 8.00 (d, *J* = 2.3 Hz, 1H), 9.92 (s, 1H), 12.78 (s, 1H); MS-FD *m/e* 377 (M⁺). Anal. (C₂₅H₂₇N₃O₃) C, H, N.

2-(4-*tert*-Butylbenzoyl)amino-4-methylsulfonylamino-*N*-(4-methoxyphenyl)benzamide (42). Using the procedure described for **48**, **41** yielded **42** (68%): ¹H NMR (DMSO-*d*₆) δ 12.27 (s, 1H), 10.31 (s, 1H), 8.57 (s, 1H), 10.30 (s, 1H), 7.92 (d, 1H, *J* = 8.7 Hz), 7.83 (d, 2H, *J* = 8.4 Hz), 7.01 (d, 1H, *J* = 8.7 Hz), 7.60–7.54 (m, 4 H), 6.93 (d, 2H, *J* = 9.0 Hz), 3.73 (s, 3H), 1.29 (s, 9 H), 3.11 (s, 3H); MS-FD *m/e* 495. Anal. Calcd for C₂₆H₂₉N₃O₅S: C, 63.09; H, 5.90; N, 8.48. Found: C, 66.12%; H, 6.08; N, 9.68%.

Preparation of 2-(4-*tert*-Butylbenzoyl)amino-5-nitro-*N*-(4-methoxyphenyl)benzamide (46). (a) **2-(4-*tert*-Butylbenzoyl)amino-5-nitrobenzoic Acid (46a).** To a mixture of 5-nitroanthranilic acid (24.6 g, 135 mmol) and pyridine (14.2 mL, 175 mmol) in *N,N*-dimethylformamide (140 mL) cooled to 0 °C was added *tert*-butylbenzoyl chloride (31.6 mL, 162 mmol). After stirring for 1 h, the reaction mixture was heated at 75 °C for 4 h, cooled, and poured into an ice/water mixture. The resulting solid was filtered, washed with water and a mixture of 1:2 diethyl ether:hexanes, and dried in vacuo at 150 °C for 2 h to give a mixture 9:1 of 2-(4-*tert*-butylbenzoyl)amino-5-nitrobenzoic acid:6-nitro-2-[4-*tert*-butylphenyl]-4*H*-3,1-benzoxazin-4-one as a light brown solid (37.1 g, 80%): mp 245–249 °C; ¹H NMR (300 MHz, DMSO-*d*₆) δ 1.32 (s, 9H), 7.63 (d, *J* = 8.7 Hz, 2H), 7.91 (d, *J* = 8.7 Hz, 2H), 8.50 (dd, *J* = 2.6, 9.0 Hz, 1H), 8.78 (d, *J* = 2.6 Hz, 1H), 8.94 (d, *J* = 9.0 Hz, 1H), 12.55 (s, 1H); MS-FD *m/e* 342. Anal. (C₁₈H₁₈N₂O₅) C, H, N.

(b) **5-Nitro-2-[4-*tert*-butylphenyl]-4*H*-3,1-benzoxazin-4-one (46b).** To a suspension of 2-(4-*tert*-butylbenzoyl)amino-5-nitrobenzoic acid, 5-nitro-2-[4-*tert*-butylphenyl]-4*H*-3,1-benzoxazin-4-one, and *N,N*-dimethylformamide (0.4 mL, 5.4 mmol) in methylene chloride (200 mL) was added oxalyl chloride (10.4 mL, 119 mmol) in a dropwise manner. After stirring for 2 h, the mixture was filtered. The filtrate was concentrated in vacuo to give **46b** as a light brown solid (32.9 g, 94%): mp 159–161 °C; ¹H NMR (300 MHz, DMSO-*d*₆) δ 1.32 (s, 9H), 7.65 (d, 2H, *J* = 8.7 Hz), 7.89 (d, 1H, *J* = 8.7 Hz), 8.16 (d, 2H, *J* = 8.7 Hz), 8.35 (dd, 1H, *J* = 8.7, 2.7 Hz), 8.75 (d, 1H, *J* = 2.7 Hz); MS-FD *m/e* 324. Anal. (C₁₈H₁₆N₂O₄) C, H, N.

(c) **2-(4-*tert*-Butylbenzoyl)amino-5-nitro-*N*-(4-methoxyphenyl)benzamide (46).** A mixture of 6-nitro-2-[4-*tert*-butylphenyl]-4*H*-3,1-benzoxazin-4-one (1.21 g, 3.73 mmol) and *p*-anisidine (551 mg, 4.47 mmol) in *N,N*-dimethylformamide (5 mL) was heated at 80 °C for 2.5 h. After cooling to room temperature, the reaction mixture was poured into an ice/water mixture and extracted twice with methylene chloride. The combined organic layers were washed with water, dried (Na₂SO₄), and filtered. The solution was concentrated and crystallized to give **46**. The mother liquor was chromatographed (silica gel, 20% diethyl ether/80% hexanes to 40% diethyl ether/60% hexanes) to yield a combined product of **46** as a light brown solid (948 mg, 56%): mp 210–211 °C; ¹H NMR δ 1.31 (s, 9H), 3.30 (s, 3H), 6.97 (d, *J* = 9.0 Hz, 2H), 7.60 (d, *J* = 9.0 Hz, 2H), 7.62 (d, *J* = 8.7 Hz, 2H), 7.87 (d, *J* = 8.7 Hz, 2H), 8.48 (dd, *J* = 2.7, 9.0 Hz, 1H), 8.84 (m, 2H), 12.31 (s, 1H); MS-FD *m/e* 447. Anal. (C₂₅H₂₅N₃O₅) C, H, N.

2-(4-*tert*-Butylbenzoyl)amino-5-amino-*N*-(4-methoxyphenyl)benzamide (47). A mixture of 2-(4-*tert*-butylbenzoyl)amino-5-nitro-*N*-(4-methoxyphenyl)benzamide (895 mg, 2.00 mmol), 10% palladium-on-carbon (90 mg) and ethyl acetate (5 mL) in ethanol (5 mL) was hydrogenated at one atmospheric pressure for 5 h. The reaction was degassed and a suspension of 10% palladium-on-carbon (45 mg) and ethyl acetate (3 mL) was added. This mixture was hydrogenated for 2 more days. The reaction was filtered through diatomaceous

earth with ethyl acetate/ethanol washes. The filtrate was concentrated in vacuo and chromatographed (silica gel, 10% ethyl acetate/90% methylene chloride to 35% ethyl acetate/65% methylene chloride) to give **47** as a white solid (487 mg, 58%): mp 212–214.5 °C; ¹H NMR δ 1.29 (s, 9H), 3.73 (s, 3H), 5.21 (br s, 2H), 6.76 (dd, J = 2.6, 9.0 Hz, 1H), 6.91 (d, J = 9.0 Hz, 2H), 6.98 (d, J = 2.6 Hz, 1H), 7.53 (d, J = 8.3 Hz, 2H), 7.59 (d, J = 9.0 Hz, 2H), 7.77 (d, J = 8.3 Hz, 2H), 8.01 (d, J = 9.0 Hz, 1H), 10.28 (s, 1H), 10.95 (s, 1H); MS-FD m/e 417. Anal. (C₂₅H₂₇N₃O₃) Calcd: C, 71.92; H, 6.52; N, 9.80. Found: C, 71.38%; H, 6.56; N, 9.80.

2-(4-tert-Butylbenzoylamino)-5-methylsulfonylamino-N-(4-methoxyphenyl)benzamide (48). To a solution of **47** (150 mg, 0.36 mmol) in methylene chloride (5 mL) at 0 °C was added pyridine (32 mL, 0.40 mmol) followed by methanesulfonyl chloride (31 μ L, 0.40 mmol). After 5 min, the reaction mixture was allowed to warm to rt and stirred for 30 min. The reaction mixture was diluted with methylene chloride and washed twice with water. The organic layer was dried (Mg-SO₄), filtered, and concentrated in vacuo. The residue was chromatographed (silica gel, 30% ethyl acetate/70% methylene chloride) to give **48** (130 mg, 73%): ¹H NMR (DMSO-*d*₆) δ 1.29 (s, 9H), 3.04 (s, 3H), 3.73 (s, 3H), 6.93 (d, 2H, J = 8.7 Hz), 7.39 (d, 1H, J = 8.7 Hz), 7.56 (d, 4H, J = 7.8 Hz), 7.61 (s, 1H), 7.80 (d, 2H, J = 7.8 Hz), 8.31 (d, 1H, J = 9.00 Hz), 9.81 (s, 1H), 10.47 (s, 1H), 11.24 (s, 1H); MS-FD m/e 495. Anal. (C₂₆H₂₉N₃O₅S·0.50H₂O) C, H, N: calcd, 8.33; found, 7.89.

Preparation of 2-(4-(Dimethylamino)benzoylamino)-4-amino-N-(4-methoxyphenyl)benzamide (52). (a) **2-(4-(Dimethylamino)benzoylamino)-4-nitro-N-(4-methoxyphenyl)benzamide (52a).** Using a procedure described for **21**, **40a** and 4-dimethylaminobenzoic acid yielded **52a** (88%): ¹H NMR (300 MHz, DMSO-*d*₆) δ 3.01 (s, 6H), 3.76 (s, 3H), 6.81 (d, J = 9.15 Hz, 2H), 6.98 (d, J = 9.15 Hz, 2H), 7.63 (d, J = 9.15 Hz, 2H), 7.77 (d, J = 9.15 Hz, 2H), 8.02 (dd, J = 2.2, 8.8 Hz, 1H), 8.15 (d, J = 8.8 Hz, 1H), 9.45 (d, J = 2.20 Hz, 1H), 10.71 (s, 1H), 11.76 (s, 1H); FIA-MS m/e 433.4 (M - 1). Anal. (C₂₃H₂₂N₄O₅) C, H, N.

(b) **2-(4-(Dimethylamino)benzoylamino)-4-amino-N-(4-methoxyphenyl)benzamide (52).** Using procedure described in **6b**, **52a** was reduced with 10% Pd/C in 20% EtOH/EtOAc to give **52** (66%): ¹H NMR (300 MHz, DMSO-*d*₆) δ 2.99 (s, 6H), 3.75 (s, 3H), 5.92 (s, 2H), 6.31 (dd, J = 2.20, J = 8.78 Hz, 1H), 6.79 (d, J = 8.78 Hz, 2H), 6.93 (d, J = 8.78 Hz, 2H), 7.55 (d, J = 9.15 Hz, 2H), 7.70 (d, J = 8.78 Hz, 1H), 7.76 (d, J = 9.15 Hz, 2H), 8.01 (d, J = 1.83 Hz, 1H), 9.89 (s, 1H), 12.55 (s, 1H); FIA-MS m/e 405.6 (M + H). Anal. (C₂₃H₂₄N₄O₃·0.25H₂O) C, H, N.

Preparation of 2-(4-(Dimethylamino)benzoylamino)-5-amino-N-(4-methoxyphenyl)benzamide (53). (a) **2-Amino-5-nitro-N-(4-methoxyphenyl)benzamide (53a).** Using a procedure described in **16a**, 5-nitroisatoic anhydride and *p*-anisidine yielded **53a** (95%): ¹H NMR (300 MHz, DMSO-*d*₆) δ 3.75 (s, 3H), 6.84 (d, J = 9.2 Hz, 1H), 6.93 (d, J = 9.2 Hz, 2H), 7.64 (s, 2H), 7.59 (d, J = 9.2 Hz, 2H), 8.59 (d, J = 2.6 Hz, 1H), 8.06 (dd, J = 2.56, 9.2 Hz, 1H), 10.31 (s, 1H); FIA-MS m/e 288.0 (M + H). Anal. (C₁₄H₁₃N₃O₄) C, H, N.

(b) **2-(4-(Dimethylamino)benzoylamino)-5-nitro-N-(4-methoxyphenyl)benzamide (53b).** Using procedure described in **21**, **53a** and 4-dimethylaminobenzoic acid yielded **53b** (84%): ¹H NMR (300 MHz, DMSO-*d*₆) δ 3.77 (s, 3H), 3.01 (s, 6H), 6.82 (d, J = 8.8 Hz, 2H), 6.99 (d, J = 9.2 Hz, 2H), 7.62 (d, J = 8.8 Hz, 2H), 7.79 (d, J = 9.2 Hz, 2H), 8.45 (dd, J = 2.6 Hz, J = 9.2 Hz, 1H), 8.82 (d, J = 9.2 Hz, 1H), 8.84 (d, J = 2.6 Hz, 1H), 10.81 (s, 1H), 12.24 (s, 1H); FIA-MS m/e 433.4 (M - H). Anal. (C₂₃H₂₂N₄O₅) C, H, N.

(c) **2-(4-(Dimethylamino)benzoylamino)-5-amino-N-(4-methoxyphenyl)benzamide (53).** Using procedure described in **6b**, **53b** was reduced with 10% Pd/C in 20% EtOH/EtOAc to give **53** (86%): ¹H NMR (300 MHz, DMSO-*d*₆) δ 2.97 (s, 6H), 3.74 (s, 3H), 5.15 (s, 2H), 6.76 (m, 3H), 6.92 (d, J = 8.8 Hz, 2H), 6.99 (d, J = 2.2 Hz, 2H), 7.60 (d, J = 8.8 Hz, 2H), 7.70 (d,

J = 8.8 Hz, 2H), 8.05 (d, J = 8.8 Hz, 1H), 10.29 (s, 1H), 10.83 (s, 1H); FIA-MS m/e 405.4 (M + H). Anal. (C₂₃H₂₄N₄O₃·0.25H₂O) C, H, N.

2-(4-(Dimethylamino)benzoylamino)-4-methanesulfonylamino-N-(4-methoxyphenyl)benzamide (54). Using procedure described in **48**, **52** yielded **54** (27%): ¹H NMR (300 MHz, DMSO-*d*₆) δ 3.00 (s, 6H), 3.76 (s, 3H), 3.12 (s, 3H), 6.81 (d, J = 8.8 Hz, 2H), 6.98 (m, 3H), 7.58 (d, J = 8.8 Hz, 2H), 7.76 (d, J = 8.8 Hz, 2H), 7.91 (d, J = 8.8 Hz, 1H), 8.61 (d, J = 1.8 Hz, 1H), 10.24 (s, 1H), 10.29 (s, 1H), 12.12 (s, 1H); FIA-MS m/e 483.3 (M + H). Anal. (C₂₄H₂₆N₄O₅S) C, H, N.

2-(4-(Dimethylamino)benzoylamino)-5-methanesulfonylamino-N-(4-methoxyphenyl)benzamide (55). Using a procedure described for **48**, **53** yielded **55** (18%): ¹H NMR (300 MHz, DMSO-*d*₆) δ 2.99 (s, 6H), 3.75 (s, 3H), 3.04 (s, 3H), 6.78 (d, J = 9.2 Hz, 2H), 6.96 (d, J = 9.2 Hz, 2H), 7.39 (dd, J = 2.2, 9.2 Hz, 1H), 7.58 (d, J = 9.2 Hz, 1H), 7.64 (d, J = 2.2 Hz, 2H), 7.73 (d, J = 8.8 Hz, 1H), 8.41 (d, J = 8.8 Hz, 2H), 9.75 (s, 1H), 10.47 (s, 1H), 11.18 (s, 1H); FIA-MS m/e 483.3 (M + H). Anal. (C₂₄H₂₆N₄O₅S) C, H, N.

Supporting Information Available: Procedures for compounds not included in the Experimental Section. This material is available free of charge via the Internet at <http://pubs.acs.org>.

References

- (1) The principle that inhibitors of fXa can produce anticoagulant effects in blood and can produce preclinical antithrombotic effects has been demonstrated from studies of potent natural fXa inhibitors from the leech and the tick. (a) Vlasuk, G. P. Structural and Functional Characterization of Tick Anticoagulant Peptide (TAP): A Potent and Selective Inhibitor of Blood Coagulation Factor Xa. *Thromb. Haemostasis* **1993**, *70*, 212–216. (b) Vlasuk, G. P.; Ramjit, D.; Fujita, T.; Dunwiddie, C. T.; Nutt, E. M.; Smith, D. E.; Shebuski, R. J. Comparison of the In Vivo Anticoagulant Properties of Standard Heparin and the Highly Selective Factor Xa Inhibitors Antistatin and Tick Anticoagulant Peptide (TAP) in a Rabbit Model of Venous Thrombosis. *Thromb. Haemostasis* **1991**, *65*, 257–262. (c) Schaffer, L. W.; Davidson, J. T.; Vlasuk, G. P.; Dunwiddie, C. T.; Siegl, P. K. S. Selective Factor Xa Inhibition by Recombinant Antistatin Prevents Vascular Graft Thrombosis in Baboons. *Arterioscl. Thromb.* **1992**, *12*, 879–885.
- (2) Small organic molecules which reversibly inhibit fXa have also been shown to produce anticoagulant activity in plasma and antithrombotic activity in animal models. (a) Hara, T.; Yokoyama, A.; Ishihara, H.; Yokoyama, Y.; Nagahara, T.; Iwamoto, M. DX-9065a, A New Synthetic, Potent Anticoagulant And Selective Inhibitor Of Factor Xa. *Thromb. Haemostasis* **1994**, *71*, 314–319. (b) Herbert, J. M.; Bernat, A.; Dol, F.; Herault, J. P.; Crepon, B.; Lormeau, J. C. DX-9065a, A Novel, Synthetic Selective And Orally Active Inhibitor Of Factor Xa: In-Vitro And In-Vivo Studies. *J. Pharmacol. Exp. Ther.* **1996**, *276*, 1030–1038. (c) Taniuchi, Y.; Sakai, Y.; Hisamichi, H.; Kayama, M.; Mano, Y.; Sato, K.; Hirayama, F.; Koshio, H.; Matsumoto, Y.; Kawasaki, T. Biochemical and Pharmacological Characterization of YM-60828, A Newly Synthesized and Orally Active Inhibitor of Human Factor Xa. *Thromb. Haemostasis* **1998**, *79*, 543–548.
- (3) Reviews: (a) Vacca, J. P. Thrombosis and Coagulation. *Annu. Rep. Med. Chem.* **1996**, *33*, 81–90. (b) Al-Obeidi, F.; Ostrem, J. A. Factor Xa Inhibitors by Classical and Combinatorial Chemistry. *Drug Discov. Today* **1998**, *3*, 223–231. (c) Sanderson, P. E. J. Small, Noncovalent Serine Protease Inhibitors. *Med. Res. Rev.* **1999**, *19*, 179–197.
- (4) Herron, D. K.; Goodson, T., Jr.; Wiley, M. R.; Weir, L. C.; Kyle, J. A.; Yee, Y. K.; Tebbe, A. L.; Tinsley, J. M.; Mendel, D.; Masters, J. J.; Franciskovich, J. B.; Sawyer, J. S.; Beight, D. W.; Ratz, A. M.; Milot, G.; Hall, S. E.; Klimkowski, V. J.; Wikel, J. H.; Eastwood, B. J.; Townner, R. D.; Gifford-Moore, D. S.; Craft, T. J.; Smith, G. 1,2-Dibenzamido benzene Inhibitors of Human Factor Xa. *J. Med. Chem.* **2000**, *43*, 859–872.
- (5) Heck, R. F.; Ziegler, C. B. Palladium-catalyzed vinylic substitution with highly activated aryl halides. *J. Org. Chem.* **1978**, *43*, 2941–2946.
- (6) Manhas, M. S.; Amin, S. G.; Rao, V. V. Heterocyclic Compounds; IX. A Facile Synthesis Of Methaqualone And Analogues. *Synthesis* **1977**, 309–310.
- (7) Zentmyer, D. T.; Wagner, E. C. The So-Called Acylantranilids (3,1,4-Benzoxazones). I. Preparation; Reactions With Water, Ammonia, And Aniline; Structure. *J. Org. Chem.* **1949**, *14*, 967–981.

- (8) Pavlidis, V. H.; Perry, P. J. The Synthesis Of A Novel Series Of Substituted 2-Phenyl-4*H*-3,1-Benzoxazin-4-ones. *Synth. Commun.* **1994**, *24*, 533–548.
- (9) Cram, D. J. Preorganization – From Solvents To Spherands. *Angew Chem. Int. Ed. Engl.* **1986**, *25*, 1039–1057.
- (10) Kollman, P. A. The Nature Of The Drug-Receptor Bond. In *Burgers Medicinal Chemistry*, 4th ed.; Wolff, M. E., Ed.; pp 322, 319.
- (11) Wiley, M. R.; Weir, L. C.; Briggs, S.; Bryan, N.; Buben, J.; Campbell, C.; Chirgadze, N. Y.; Conrad, R. C.; Craft, T. J.; Ficorilli, J. V.; Franciskovich, J. B.; Froelich, L. L.; Gifford-Moore, D. S.; Goodson, T., Jr.; Herron, D. K.; Klimkowski, V. J.; Kurz, K. D.; Kyle, J. A.; Masters, J. J.; Ratz, A. M.; Milot, G.; Shuman, R. T.; Smith, T.; Smith, G. F.; Tebbe, A. L.; Tinsley, J. M.; Towner, R. D.; Wilson, A.; Yee, Y. K. Structure-Based Design of Potent, Amidine-Derived Inhibitors of Factor Xa: Evaluation of Selectivity, Anticoagulant Activity, and Antithrombotic Activity. *J. Med. Chem.* **2000**, *43*, 883–899.
- (12) (a) Sall, D. J.; Bastian, J. A.; Briggs, S. L.; Buben, J. A.; Chirgadze, N. Y.; Clawson, D. K.; Denny, M. L.; Giera, D. D.; Gifford-Moore, D. S.; Harper, R. W.; Hauser, K. L.; Klimkowski, V. J.; Kohn, T. J.; Lin, H.; McCowan, J. R.; Palkowitz, A. D.; Smith, G. F.; Takeuchi, K.; Thrasher, K. J.; Tinsley, J. M.; Utterback, B. G.; Yan, S. B.; Zhang, M. Dibasic Benzo[b]-thiophene Derivatives As A Novel Class Of Active Site-Directed Thrombin Inhibitors. *J. Med. Chem.* **1997**, *40*, 3489–3493. (b) Smith, G. F.; Shuman, R. T.; Craft, T. J.; Gifford, D. S.; Kurz, K. D.; Jones, N. D.; Chirgadze, N.; Hermann, R. B.; Coffman, W. J.; Sandusky, G. E.; Roberts, E.; Jackson, C. V. A Family of Arginal Thrombin Inhibitors Related to Efegatran. *Semin. Thromb. Hemostasis* **1996**, *22*, 173–183.
- (13) Smith, G. F.; Gifford-Moore, D. S.; Craft, T. J.; Chirgadze, N.; Ruterbories, K. J.; Lindstrom, T. D.; Satterwhite, J. H. Efegatran: A New Cardiovascular Anticoagulant. In *New Anticoagulants for the Cardiovascular Patient*; Pifarre, R., Ed.; Hanley & Belfus, Inc.: Philadelphia, 1997; pp 265–300.
- (14) Padmanabhan, K.; Padmanabhan, K. P.; Tulinsky, A.; Park C. H.; Bode, W.; Huber, R.; Blankenship, D. T.; Cardin, A. D.; Kisiel, W. Structure of Human Des(1–45) Factor Xa at 2.2 Å Resolution. *J. Mol. Biol.* **1993**, *232*, 947–966.
- (15) Molecular Simulations Inc., 9685 Scranton Rd., San Diego, CA 92121.
- (16) Brooks, B. R.; Brucoleri, R. E.; Olafson, B. D.; States, D. J.; Swaminathan, S.; Karplus, M. CHARMM: A Program for Macromolecular Energy, Minimization, and Dynamics Calculations. *J. Comput. Chem.* **1983**, *4*, 187–217.
- (17) Henderson, P. J. F. A Linear Equation that Describes the Steady-State Kinetics of Enzymes and Subcellular Particles Interacting with Tightly Bound Inhibitors. *Biochem. J.* **1972**, *127*, 321–333.
- (18) Bieth, J. G. Pathophysiological Interpretation of Kinetic Constants of Protease Inhibitors. *Bull. Eur. Physiopath. Resp.* **1980**, *16* (Suppl.), 183–195.

JM990327E